Inorganic Chemistry

Communication

pubs.acs.org/IC

Polymorphism-Dependent Spin-Crossover: Hysteretic Two-Step Spin Transition with an Ordered [HS−HS−LS] Intermediate Phase

Jie Luan,[†] Jian Zhou,[†] Zhan Liu,[†] Bowen Zhu,[†] Huisi Wang,[†] Xin Bao,*[,†] Wei Liu,[‡] Ming-Liang Tong,*[,‡] Guo Peng,[§] Haonan Peng,[∥] Lionel Salmon,[∥] and Azzedine Bousseksou[∥]

[†]School of Chemical Engineering and [§]Herbert Gleiter Institute of Nanoscience, Nanjing University of Science and Technology, 210094 Nanjing, P. R. China

[‡]Key Laboratory of Bioinorganic and Synthetic Chemistry of Ministry of Education, School of Chemistry and Chemical Engineering, Sun Yat-Sen University, 510275 Guangzhou, P. R. China

[∥]LCC, CNRS, Université de Toulouse (UPS, INP), 205 route de Narbonne, 31077 Toulouse, France

Supporting Information

ABSTRACT: A mononuclear iron(II) complex has been isolated in two polymorphs. Polymorph **1b** remains high-spin over all temperatures, whereas polymorph **1a** undergoes a cooperative two-step spin crossover accompanied by symmetry breaking, showing an ordered 2:1 high-spin−low-spin intermediate phase.

As one of the most attractive molecule-based switchable materials, spin-crossover (SCO) complexes have potential applications as molecular switches, data storage materials, and display devices.[1] Most frequently, SCO between high (HS) and low (LS) spin states occurs in a single step, of either complete or incomplete and abrupt or gradual type.[2] Systems exhibiting two-step SCO are of particular interest because they may serve to improve the information storage capacity. However, examples of such types, particularly those with two hysteresis loops, are quite rare.[3,4] The most common reason for a multistep transition is the presence of two structurally inequivalent SCO sites. The other possibility is the occurrence of symmetry breaking in the intermediate phase (IP).[5] In 2003, Bürgi et al. discovered that the two-step SCO in the well-studied complex $[Fe(2\text{-pic})_3]Cl_2 \cdot EtOH$ (pic = picolylamine) was accompanied by a crystallographic phase transition between a single site HS (or LS) phase and an [HS−LS] ordered IP.[5a] In 2009, Collet et al. reported a mononuclear iron(II) complex with four different phases, including a [LS−HS−HS−LS] long-range-ordered IP.[5c] In contrast, Reedjik et al. synthesized a two-step SCO iron(II) complex whose IP consists of ordered [HS−LS−LS] motifs and is stable over a large temperature range.[4] The unequal populations of the HS and LS states with long-range ordering in the IP are quite rare and have only been reported for a few examples. In 2011, Müller-Bunz et al. reported an example of concerted SCO and symmetry breaking in an iron(III) complex with a 1:2 ratio of spin states in the IP, but in that case 1:2 LS−HS.[6] Besides, IPs with ordered 1:3 HS−LS,[7] 3:1 HS−LS,[8] and 18:12 LS−HS[9] have also been observed.

In the present study, we have isolated two polymorphs (**1a** and **1b**) of the mononuclear iron(II) complex $[Fe(bpmen)(NCSe)_2]$ [bpmen = *N*,*N*′-dimethyl-*N*,*N*′-bis(2-pyridylmethyl)-1,2-ethanediamine]. **1a** undergoes a cooperative two-step SCO with thermal hysteresis, whereas **1b** remains HS over all temperatures. For **1a**, a 2:1 HS−LS population was observed in the IP and the unit cell volume becomes 3 times as large, showing long-range ordering of the [HS−HS−LS] sites.

1a and **1b** are two competing products from the 1:1:2 reaction of bpmen, $Fe(ClO_4)_2 \cdot 6H_2O$, and KNCSe in acetonitrile. They can be easily discriminated by different crystal morphologies: platelike crystals for **1a** and block crystals for **1b**.

Magnetic susceptibility data were recorded on polycrystalline samples over the temperature range 300−10 K. As shown in Figure 1, at a cooling rate of 2 K min^{-1}, the $\chi_m T$ product of **1a** is

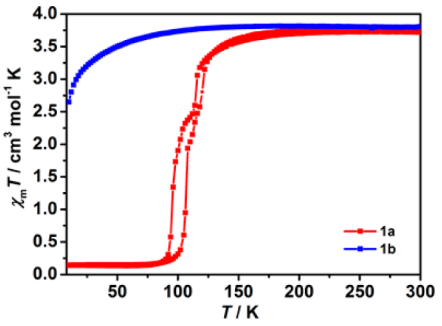

Figure 1. Variable-temperature magnetic susceptibility studies of **1a** and **1b**. Data recorded in both cooling and heating modes at a scan rate of 2 K min^{-1}.

3.7 cm^3 mol^{-1} K at 300 K and decreases slightly to 3.2 cm^3 mol^{-1} K at 118 K, indicating that the Fe^{II} ions are in HS state. Upon further cooling, the $\chi_m T$ value drops sharply to 2.5 cm^3 mol^{-1} K at 112 K, corresponding to a spin conversion of $^1/_3$ of the metal ions. A second abrupt decrease of $\chi_m T$ was observed between 103 and 90 K, from 2.2 to 0.2 cm^3 mol^{-1} K, corresponding to the SCO of the remaining $^2/_3$ of the metal ions. The measurement performed in the subsequent heating mode revealed the presence of 10 and 5 K thermal hysteresis for each step. The values of critical temperatures (the temperature of 50% spin state conversion) are $T_{c1}\downarrow$ = 115 K and $T_{c2}\downarrow$ = 96 K in the cooling mode and $T_{c1}\uparrow$ = 120 K and $T_{c2}\uparrow$ = 106 K in the warming mode.

Received: March 22, 2015
Published: May 8, 2015

DOI: 10.1021/acs.inorgchem.5b00629
Inorg. Chem. 2015, 54, 5145−5147

The SCO behavior is reproducible over successive thermal cycles (Figure S1 in the Supporting Information, SI). When the scan rate is increased to 8 K min^{-1}, the transition curve is quite similar but the hysteresis widths for the two steps increase to 16 and 10 K, respectively (Figure S2 in the SI). In contrast, **1b** remains in the HS state in the temperature range studied. The $\chi_m T$ value of **1b** at 300 K is 3.8 cm^3 mol^{-1} K, lying in the range typically observed for the HS Fe^{II} ion. The drop of $\chi_m T$ below 50 K is probably due to the zero-field-splitting and spin−orbit coupling effect.

1a shows a striking color change associated with SCO, from bright yellow at room temperature to dark red at liquid-nitrogen temperature (Figure S3 in the SI). This effect is attributed to the reversible bleaching of the characteristic $^1A_1 \rightarrow {}^1T_1$ absorption band centered around λ = 550 nm. We thus investigated the change in the optical reflectance at the specific wavelength of 543 nm. Thermal variation of the reflectance is in good agreement with the magnetic curve (Figure S3 in the SI). Upon cooling, the signal decreases in two relatively abrupt steps centered at 114 and 97 K, respectively. The subsequent warming results in a 4 K wide hysteresis for the lower temperature transition.

^{57}Fe Mössbauer spectra of **1a** were recorded at 150, 110, and 80 K in the cooling mode (Figure 2 and Table S1 in the SI). The

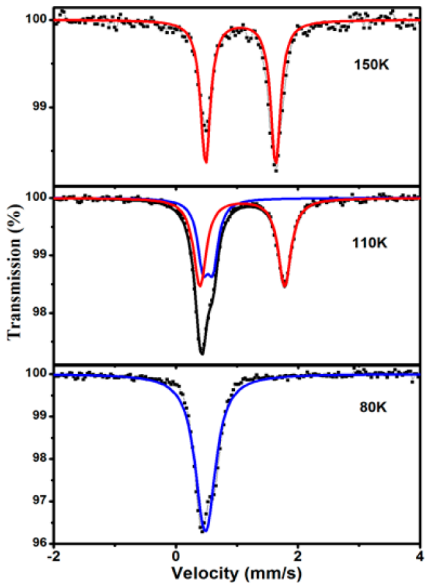

Figure 2. ^{57}Fe Mössbauer spectra of **1a** recorded at 150, 110, and 80 K in the cooling mode. The spectra are deconvoluted into HS (red line) and LS (blue line) sites.

spectrum at 150 K consists of a unique quadrupole doublet with an isomer shift of δ = 1.06 mm s^{-1} and a quadrupole splitting of ΔE_Q = 1.14 mm s^{-1}, which is characteristic of a HS Fe^{II} ion. Upon cooling to 110 K, the spectrum consists of two doublets in a 63.6:36.4 ratio. The isomer shift and quadrupole splitting corresponding to the HS Fe^{II} ion are 1.08 and 1.38 mm s^{-1} respectively. The other doublet with values of δ = 0.52 mm s^{-1} and ΔE_Q = 0.16 mm s^{-1} is assigned to the LS state. The spectrum at 80 K shows a doublet with parameters of δ = 0.48 mm s^{-1} and $\Delta E_Q \approx$ 0.1 mm s^{-1}, denoting a complete SCO to the LS state. The observed asymmetry in the quadrupole doublet probably arises from the anisotropy of crystalline samples.

Polymorph **1a** crystallizes in the orthorhombic space group *Aba*2, while polymorph **1b** crystallizes in the monoclinic space group *C*2/*c*. Their molecular structures are comparable to those of the previously reported complexes constructed with similar tetradentate ligands. The occurrence of SCO in those complexes indicates the appropriate ligand-field strength of such types of ligands.[5h,10] As shown in Figure 3, the tetradentate ligand in both

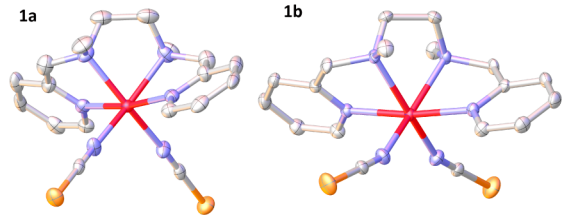

Figure 3. View of the molecular structures of **1a** (left) and **1b** (right) in HS states. Color code: C, gray; Fe, red; Se, orange; N, blue. H atoms are omitted for clarity.

polymorphs adopts a *cis*-α conformation with pyridine groups in the axial positions, leaving two cis positions for NCSe coligands. In the HS state (measured at 150 K for **1a** and 173 K for **1b**), the asymmetric units of **1a** and **1b** contain half of the molecule with a 2-fold axis passing through the Fe^{II} atom. The average Fe−N bond lengths in **1a** and **1b** are 2.16 and 2.19 Å, respectively. The Fe−N≡C angle is 168.9° in **1a** and 159.3° in **1b**. The larger deviation from 180° indicates a weaker σ bond and hence a weaker ligand field strength. The octahedral environment of **1b** is slightly distorted (Σ = 84.5°) from that of **1a** (Σ = 75.7°).

Upon cooling to 100 K, the unit cell volume of **1a** triples, and consequently the asymmetric unit now contains one and a half molecules (Figures 4 and S4 in the SI). The average Fe−N bond

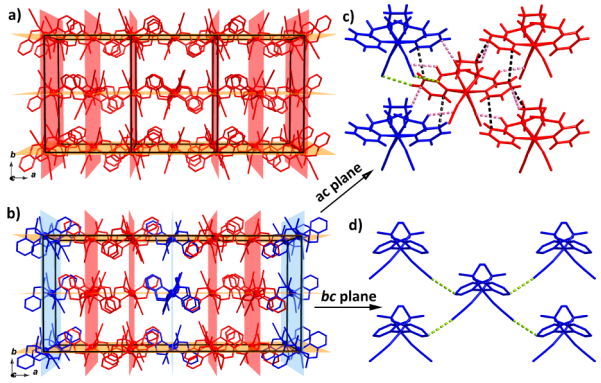

Figure 4. Central projection of crystal packings for **1a** in the HS phase (a) and IP (b). HS and LS molecules are drawn in red and blue, respectively. 2D supramolecular layers are in the *ac* (c) and *bc* (d) planes. Short contacts are indicated as dotted lines.

length in the full occupancy molecule (2.17 Å) is typical for the HS Fe^{II} ion, whereas that in the half occupancy molecule (2.00 Å) matches the Fe^{II} ion in the LS state. The IP is thus stabilized in the unusual ordered [HS−HS−LS] state. The octahedral distortion parameter Σ value for the LS Fe^{II} ion decreases significantly to 43.1°, revealing a local rearrangement to a more regular geometry upon SCO. Upon further cooling to 95 K, new supercell reflections appear and the unit cell volume changes to 2 times over that at 150 K (Table S2 and Figure S10 in the SI). Unfortunately, the crystals cracked after several minutes, and it was not possible to determine the X-ray structure.

The crystal packing of **1a** remains similar in the HS phase and IP. As shown in Figure 4, the 2D supramolecular layer in the *ac*

DOI: 10.1021/acs.inorgchem.5b00629
Inorg. Chem. 2015, 54, 5145−5147

plane has a close packing with abundant Se···H, C···C, and C···H short contacts, while in the *bc* plane, only Se···C van der Waals interactions were found. Upon SCO to IP, HS and LS sites coexist in the close-packed *ac* layer, while either HS or LS ions locate in the loose-packed *bc* layer, resulting in an alternative arrangement of one LS and two HS layers along the *a* axis. Compared with the HS phase, Se···C contacts become weaker in the LS layer but stronger in the HS layer; in the *ac* plane, short contacts become stronger and several new short contacts appear (Figures S5 and S6 and Table S4 in the SI). Those differences in the two planes may play a subtle role in stabilizing **1a** in an ordered mixed-spin state. In **1b**, a similar 2D layer connected by Se···H short contacts was found in the *ab* plane. $\pi-\pi$ interactions and C···H van der Waals interactions between adjacent layers lead to a 1D supramolecular chain (Figure S7 in the SI). Different crystal packings between **1a** and **1b** should also contribute to their different magnetic behaviors.

In conclusion, the mononuclear iron(II) complex [Fe(bpmen)$(NCSe)_2$] has been found to show polymorphism-dependent magnetic properties. The coordination orientation of the NCSe ligand plays an important role in stabilizing the two polymorphs in different spin states. Polymorph **1a** provides a rare example showing hysteretic two-step SCO accompanied by a color change. In particular, a 2:1 rather than a 1:1 HS−LS population in the IP was confirmed by both magnetic and structural studies. X-ray diffraction data evidence a crystallographic phase transition in the IP with a tripled unit cell. One LS and two HS layers propagate along the *a* axis alternatively, resulting in an unusual ordered [HS−HS−LS] state.

■ ASSOCIATED CONTENT

Supporting Information

Experimental procedures, crystallographic data in CIF format, powder X-ray diffraction, figures showing crystal packings and diffraction patterns, and ^{57}Fe Mössbauer parameters. The Supporting Information is available free of charge on the ACS Publications website at DOI: 10.1021/acs.inorgchem.5b00629.

■ AUTHOR INFORMATION

Corresponding Authors

*E-mail: baox199@126.com.

*E-mail: tongml@mail.sysu.edu.cn.

Notes

The authors declare no competing financial interest.

■ ACKNOWLEDGMENTS

This work was supported by the National Natural Science Foundation of China (Grant 21401104), the Natural Science Foundation of Jiangsu Province (Grant BK20140774), the Fundamental Research Funds for the Central Universities (Grant 30920140111002), and financial support from State Key Laboratory of Coordination Chemistry of Nanjing University and the Zijin Intelligent Program of NJUST.

■ REFERENCES

(1) (a) Kahn, O.; Martinez, C. J. *Science* **1998**, *279*, 44−48. (b) Gütlich, P.; Garcia, Y.; Woike, T. *Coord. Chem. Rev.* **2001**, *219*, 839−879. (c) Gütlich, P.; Ksenofontov, V.; Gaspar, A. B. *Coord. Chem. Rev.* **2005**, *249*, 1811−1829. (d) Real, J. A.; Gaspar, A. B.; Muñoz, M. C. *Dalton Trans.* **2005**, 2062−2079. (e) Sato, O.; Tao, J.; Zhang, Y.-Z. *Angew. Chem., Int. Ed.* **2007**, *46*, 2152−2187.

(2) (a) Gütlich, P.; Goodwin, H. A. Spin Crossover in Transition Metal Compounds I−III. *Topics in Current Chemistry*; Springer: Berlin, 2004; Vols. *233*−*235*. (b) Bousseksou, A.; Molnár, G.; Salmon, L.; Nicolazzi, W. *Chem. Soc. Rev.* **2011**, *40*, 3313−3335. (c) Halcrow, M. A. *Spin-crossover Materials: Properties and Applications*; John Wiley & Sons: New York; 2013. (d) Halcrow, M. A. *Chem. Soc. Rev.* **2011**, *40*, 4119−4142. (e) Olguin, J.; Brooker, S. *Coord. Chem. Rev.* **2011**, *255*, 203−240. (f) Gaspar, A. B.; Seredyuka, M. *Coord. Chem. Rev.* **2014**, *268*, 41−58.

(3) (a) Boinnard, D.; Bousseksou, A.; Dworkin, A.; Savariault, J. M.; Varret, F.; Tuchagues, J. P. *Inorg. Chem.* **1994**, *33*, 271−281. (b) Ksenofontov, V.; Gaspar, A. B.; Niel, V.; Reiman, S.; Real, J. A.; Gütlich, P. *Chem.—Eur. J.* **2004**, *10*, 1291−1298. (c) Li, Z.-Y.; Dai, J.-W.; Gagnon, K. J.; Cai, H.-L.; Yamamoto, T.; Einaga, Y.; Zhao, H.-H.; Kanegawa, S.; Sato, O.; Dunbar, K. R.; Xiong, R.-G. *Dalton Trans.* **2013**, *42*, 14685−14688. (d) Bao, X.; Shepherd, H. J.; Salmon, L.; Molnár, G.; Tong, M.-L.; Bousseksou, A. *Angew. Chem., Int. Ed.* **2013**, *52*, 1198−1202. (e) Aravena, D.; Castillo, Z. A.; Muñoz, M. C.; Gaspar, A. B.; Yoneda, K.; Ohtani, R.; Mishima, A.; Kitagawa, S.; Ohba, M.; Real, J. A.; Ruiz, E. *Chem.—Eur. J.* **2014**, *20*, 12864−12873. (f) Klein, Y. M.; Sciortino, N. F.; Ragon, F.; Housecroft, C. E.; Kepert, C. J.; Neville, S. M. *Chem. Commun.* **2014**, *50*, 3838−3840.

(4) Bonnet, S.; Siegler, M. A.; Costa, J. S.; Molnár, G.; Bousseksou, A.; Spek, A. L.; Gamez, P.; Reedijk, J. *Chem. Commun.* **2008**, 5619−5621.

(5) (a) Chernyshov, D.; Hostettler, M.; Törnroos, K. W.; Bürgi, H.-B. *Angew. Chem., Int. Ed.* **2003**, *42*, 3825−3830. (b) Yamada, M.; Hagiwara, H.; Torigoe, H.; Matsumoto, N.; Kojima, M.; Dahan, F.; Tuchagues, J.-P.; Re, N.; Iijima, S. *Chem.—Eur. J.* **2006**, *12*, 4536−4549. (c) Brefuel, N.; Watanabe, H.; Toupet, L.; Come, J.; Matsumoto, N.; Collet, E.; Tanaka, K.; Tuchagues, J.-P. *Angew. Chem., Int. Ed.* **2009**, *48*, 9304−9307. (d) Sato, T.; Nishi, K.; Iijima, S.; Kojima, M.; Matsumoto, N. *Inorg. Chem.* **2009**, *48*, 7211−7229. (e) Sheu, C.-F.; Chen, S.-M.; Wang, S.-C.; Lee, G.-H.; Liu, Y.-H.; Wang, Y. *Chem. Commun.* **2009**, 7512−7514. (f) Cointe, M. B.; Moussa, N. O.; Tzrop, E.; Moréac, A.; Molnár, G.; Toupet, L.; Bousseksou, A.; Létard, J.-F.; Matouzenko, G. S. *Phys. Rev. B* **2010**, *82*, 214106−1−11. (g) Nihei, M.; Tahira, H.; Takahashi, N.; Otake, Y.; Yamamura, Y.; Saito, K.; Oshio, H. *J. Am. Chem. Soc.* **2010**, *132*, 3553−3560. (h) Lennartson, A.; Bond, A.; Piligkos, S.; McKenzie, C. *Angew. Chem., Int. Ed.* **2012**, *51*, 11049−11052. (i) Lin, J.-B.; Xue, W.; Wang, B.-Y.; Tao, J.; Zhang, W.-X.; Zhang, J.-P.; Chen, X.-M. *Inorg. Chem.* **2012**, *51*, 9423−9430. (j) Vieira, B. J. C.; Coutinho, J. T.; Santos, I. C.; Pereira, L. C. J.; Waerenborgh, J. C.; da Gama, V. *Inorg. Chem.* **2013**, *52*, 3845−3850. (k) Li, Z.-Y.; Dai, J. W.; Shiota, Y.; Yoshizawa, K.; Kanegawa, S.; Sato, O. *Chem.—Eur. J.* **2013**, *19*, 12948−12952. (l) Kusz, J.; Nowak, M.; Gütlich, P. *Eur. J. Inorg. Chem.* **2013**, 832−842.

(6) Griffin, M.; Shakespeare, S.; Shepherd, H. J.; Harding, C. J.; Létard, J.-F.; Desplanches, C.; Goeta, A. E.; Howard, J. A. K.; Powell, A. K.; Mereacre, V.; Garcia, Y.; Naik, A. D.; Müller-Bunz, H.; Morgan, G. G. *Angew. Chem., Int. Ed.* **2011**, *50*, 896−900.

(7) Sciortino, N. F.; Scherl-Gruenwald, K. R.; Chastanet, G.; Halder, G. J.; Chapman, K. W.; Létard, J.-F.; Kepert, C. J. *Angew. Chem., Int. Ed.* **2012**, *51*, 10154−10158.

(8) Murnaghan, K. D.; Carbonera, C.; Toupet, L.; Griffin, M.; Dîrtu, M. M.; Desplanches, C.; Garcia, Y.; Collet, E.; Létard, J.-F.; Morgan, G. G. *Chem.—Eur. J.* **2014**, *20*, 5613−5618.

(9) Brefuel, N.; Collet, E.; Watanabe, H.; Kojima, M.; Matsumoto, N.; Toupet, L.; Tanaka, K.; Tuchagues, J.-P. *Chem.—Eur. J.* **2010**, *16*, 14060−14068.

(10) Létard, J.-F.; Asthana, S.; Shepherd, H. J.; Guionneau, P.; Goeta, A. E.; Suemura, N.; Ishikawa, R.; Kaizaki, S. *Chem.—Eur. J.* **2012**, *18*, 5924−5934.

DOI: 10.1021/acs.inorgchem.5b00629
Inorg. Chem. 2015, 54, 5145−5147